

Histone Deacetylase Inhibitors through Click Chemistry

Jie Shen,^{†,||} Robert Woodward,^{†,||} James Patrick Kedenburg,[†] Xianwei Liu,[‡] Min Chen,[‡] Lanyan Fang,[§] Duxin Sun,[§] and Peng George Wang^{*,†}

Departments of Biochemistry and Chemistry, The Ohio State University, 876 Biological Sciences Building, 484 West 12th Avenue, Columbus, Ohio 43210, Division of Pharmaceutics, School of Pharmacy, The Ohio State University, 500 West 12th Avenue, Columbus, Ohio 43210, College of Life Science, Shandong University, Jinan, Shandong, 250100, P.R. China

Received May 8, 2008

Histone deacetylase inhibitors (HDACi) are a relatively new class of chemotherapy agents. Herein, we report a click-chemistry based approach to the synthesis of HDACi. Fourteen agents were synthesized from the combination of two alkyne and seven azido precursors. The inhibition of HDAC1 and HDAC8 was then determined by in vitro enzymatic assays, after which the cytotoxicity was evaluated in the NCI human cancer cell line screen. A lead compound **5g** (NSC746457) was discovered that inhibited HDAC1 at an IC₅₀ value of 104 ± 30 nM and proved quite potent in the cancer cell line screen with GI₅₀ values ranging from 3.92 μM to 10 nM. Thus, this click HDACi design has provided a new chemical scaffold that has not only revealed a lead compound, but one which is easily amendable to further structural modifications given the modular nature of this approach.

Introduction

Posttranscriptional modifications of histones are important processes in epigenetics.^{1–3} The reversible acetylation of Lys residues,^{4–6} for example, can help control the remodeling status of chromatin via charge–charge interactions between negatively charged DNA and neutral or positively charged histones. The removal and addition of these acetyl groups is catalyzed by the enzymes histone deacetylase (HDAC⁴) and histone acetyltransferase (HAT), respectively. In the past 10 years, studies on this process have attracted an increasing amount of attention, due in part to the observations that aberrant hypoacetylation of histones frequently occurs in tumor cells, resulting in the silencing of specific (tumor suppressor) genes.⁷ Accordingly, clinical and biological studies have shown that inhibition of HDACs can selectively inhibit cancer cell growth.⁸ It has also been revealed that HDACs have a panel of nonhistone targets, many of which are involved in tumorigenesis.^{9–17} All of these features thus establish HDAC as an attractive target in cancer chemotherapy.^{18–21}

Thus far, 18 human HDAC subtypes have been identified and accordingly divided into four classes based upon their homology to yeast HDACs.²⁰ Class I (yeast transcriptional regulator RPD3) and II (yeast Hda 1) HDACs require a zinc ion to mediate deacetylation and are therefore mechanistically different from the class III (SIR2 yeast family) NAD⁺ dependent HDACs. While HDAC 11 possesses similar catalytic activity to classes I and II HDACs in terms of requiring a zinc ion, it actually serves as the sole member of class IV due to low overall sequence similarity with classes I and II.

In the case of the aforementioned Zn(II) dependent HDAC isozymes, the active site structure was first revealed by a

homologue of the hyperthermophilic bacterium *Aquifex aeolicus* in 1999.²² In general, the active site is a tube-like pocket that accommodates the side chain of client Lys residues. Located at the bottom of this pocket is the Zn(II) cofactor, which acts as a Lewis acid to catalyze hydrolysis of the acetylated Lys side chain. The opening region (also called the cap region) of the active site consists of multiple loops and is thus highly malleable.

From this elucidation of the structure of the HDAC active site, progress on HDACi design has been greatly facilitated (Figure 1). In most cases, the reported inhibitor is composed of the following three moieties: a Zn(II) binding moiety, a spacer moiety, and a “cap” moiety. Of the demonstrated Zn(II) binding moieties, the hydroxamic acid (HA) functionality is the most common. For example, the HA moiety exists in the naturally occurring compound TSA as well as in the clinically approved drug SAHA. In spite of the strong affinity of HA with Zn(II), however, the in vivo efficacy of HA-containing HDACi is impaired by the short clearance time of these agents.^{23–25} Therefore, non-HA HDACi design has been explored.^{26,27} These non-HA moieties include electrophilic ketones (e.g., **1** in Figure 1), *O*-aminoanilides (e.g., MS-275), thiols (or the pro-drug forms) (e.g. FK-228 and **2**), and a variety of others. However, in terms of binding affinity, none are as strong as HA. As for the spacer moiety, proper length is the key factor in successful HDAC inhibition. For example, for SAHA and its analogues, six CH₂ units are preferred, whereas chiral-center-and-HA-containing HDACi (e.g., CHAPs and **3**) prefer five CH₂ units between the HA and the chiral center.^{28–30} Similarly, chiral-center-and-thiol-containing HDACi (e.g., **2**) prefer five CH₂ units in the spacer moiety. In addition to these length requirements, introduction of an unsaturated moiety within the spacer region has also proved to be a valuable feature in enhancing potency (e.g., TSA, MS275, (S)-HDAC-42 and **4**). Such value appears to arise from π–π stacking interactions between the unsaturated moiety and two conserved Phe residues that occur near the midpoint of the tube-like pocket (for HDAC8, they are Phe152 and Phe208) in the 11 Zn(II) dependent human HDACs.³¹ In regards to the “cap” moiety, a hydrophobic substituent, especially an aromatic substituent, is frequently

* To whom correspondence should be addressed. Phone: (+1) 614-292-9884. Fax: (+1) 614-688-3106. E-mail: wang.892@osu.edu.

[†] Departments of Biochemistry and Chemistry, The Ohio State University.

[‡] Shandong University.

[§] School of Pharmacy, The Ohio State University.

^{||} Authors who contributed equally to this paper.

^α Abbreviations: HDAC, histone deacetylase; HDACi, histone deacetylase inhibitor; SAHA, Suberoylanilide hydroxamic acid; TSA, trichostatin A; HA, hydroxamic acid.

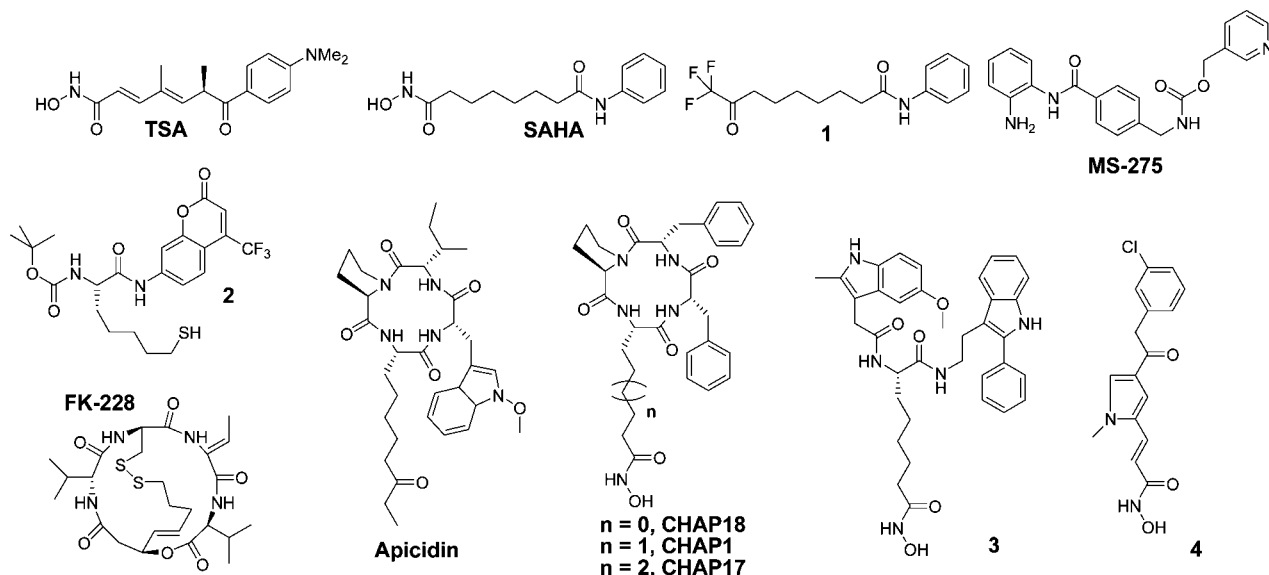


Figure 1. Current HDACi.

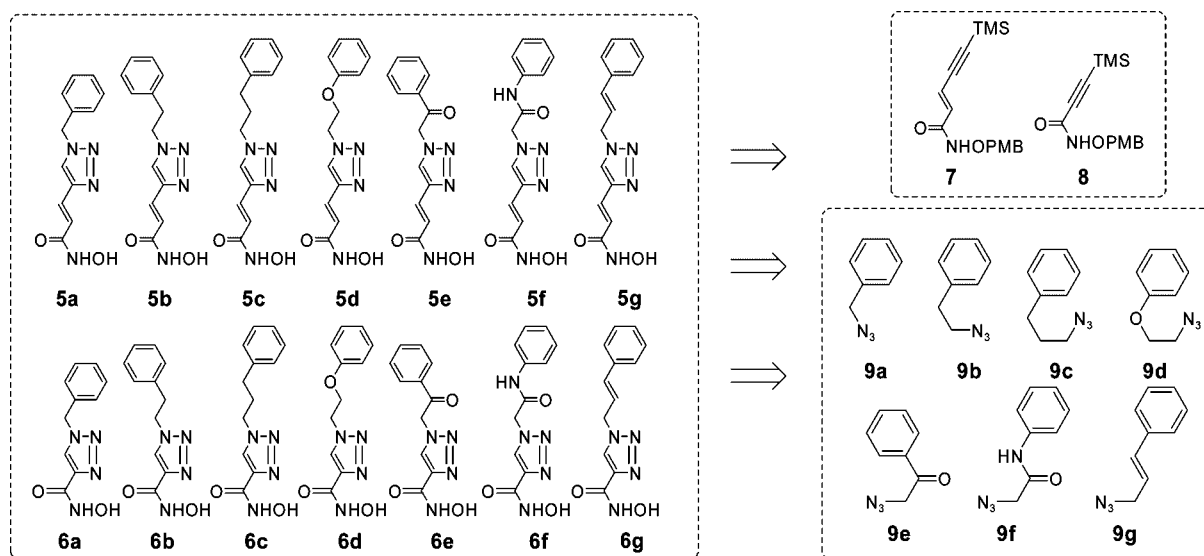


Figure 2. Combinatorial Design of HDACi via Click Chemistry.

incorporated. It should be noted that structure derivatization at the “cap” region is a key strategy in current HDACi design because topological differences are observed in the corresponding “cap” regions of HDAC isozymes.

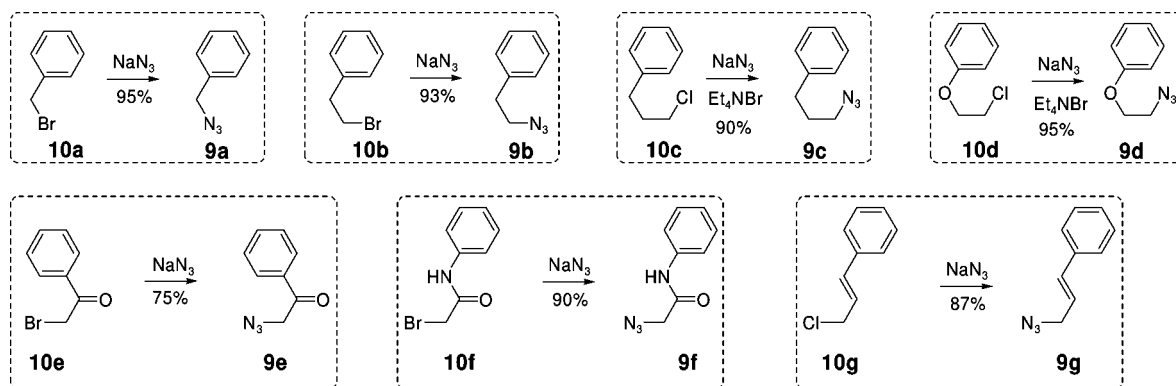
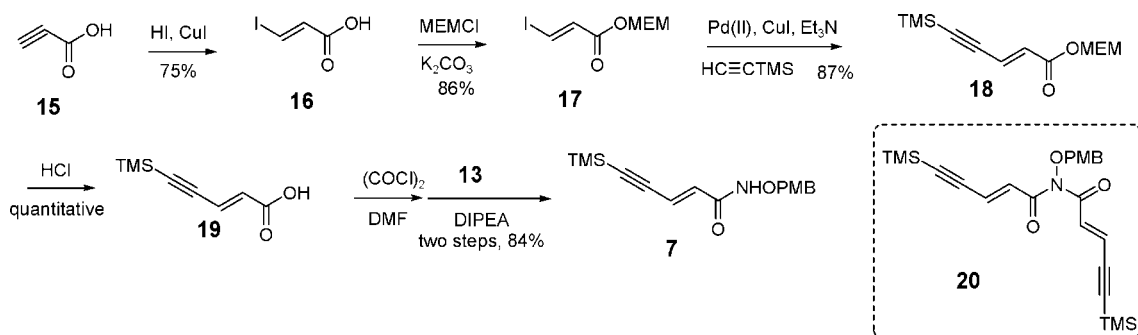
Herein, we report a HDACi scaffold that is built upon a Huisgen 1,3-dipolar cycloaddition of alkyne and azido precursors (Figure 2). This reaction has been widely applied in chemical synthesis in recent years in efforts to develop new drugs.^{32–35} It is now recognized as the premier example of the click reaction due to the convenient availability and high stability of the alkyne and azide precursors, as well as the mild reaction conditions and nearly quantitative yields. In our design, the precursors corresponding to the “cap” moiety of the HDACi contain an azido group, whereas the zinc chelating functionality precursors contain an alkyne group. The “clicked” products have a triazole ring in the spacer moiety, which may enhance the HDAC binding affinity via π – π stacking interactions. We have accordingly named these HDACi as click HDACi. Currently, 14 click HDACi (**5a–f** and **6a–f**) have been prepared from two alkyne precursors (**7** and **8**) and seven azido-substituted precursors (**9a–g**) via this combinatorial approach. From these

14 HDACi, a lead compound, **5g**, was discovered that exhibited an in vitro potency comparable to that of SAHA which was clinically approved in 2007 as a chemotherapy agent.

Results and Discussion

The seven azido precursors **9a–g** (Scheme 1) were synthesized from the corresponding halide substrates **10a–g** via treatment with 0.5 M sodium azide in DMSO (Scheme 1).³⁶ All products, with the exceptions of **9c** and **9d**, were obtained after overnight stirring. In the case of **9e**, however, the reaction had to be carried out at 0 °C to provide satisfactory yields. For **9c** and **9d**, tetraethylammonium bromide was added to catalyze the reactions, which were subsequently complete after two days. Excluding **9e**, all products could be used directly in the following steps without column purification.

The preparation of the alkyne precursor **8** began with the synthesis of the PMB-protected hydroxylamine **13** via established procedures (Scheme 2).³⁷ Subsequent amidation of **13** with the commercially available acid **14** provided intermediate **8** in 61% yield.

Scheme 1. Preparation of the Azido Precursors **9a–g**Scheme 2. Preparation of Alkyne Precursor **8**Scheme 3. Preparation of Alkyne Precursor **7**

In contrast, synthesis of the alkyne precursor **7** (Scheme 3) was initiated through conversion of the propionic acid **15** to the *trans*-iodopropionic acid **16** in 75% yield according to reported procedures.³⁸ The synthesis of **18** from **16** utilizing a known route, which was employed to prepare the corresponding (*Z*)-isomer.³⁹ This route entailed initial protection of the acid **16** with MEMCl to furnish the ester **17** (86% yield). **18** was subsequently obtained in 87% yield via a Sonogashira reaction. Deprotection of **18** with HCl to afford **19** (quantitative), followed by treatment with oxalyl chloride and a catalytic amount of DMF, yielded an acid chloride intermediate. This acid chloride was used directly in the next step in which DIPEA and **13** (2: 1) were added within 1 min at $-10\text{ }^{\circ}\text{C}$ to give **7** in 84% yield. Such rapid addition of the amine **13** was necessary as slow addition dramatically increased the yield of the byproduct **20**.

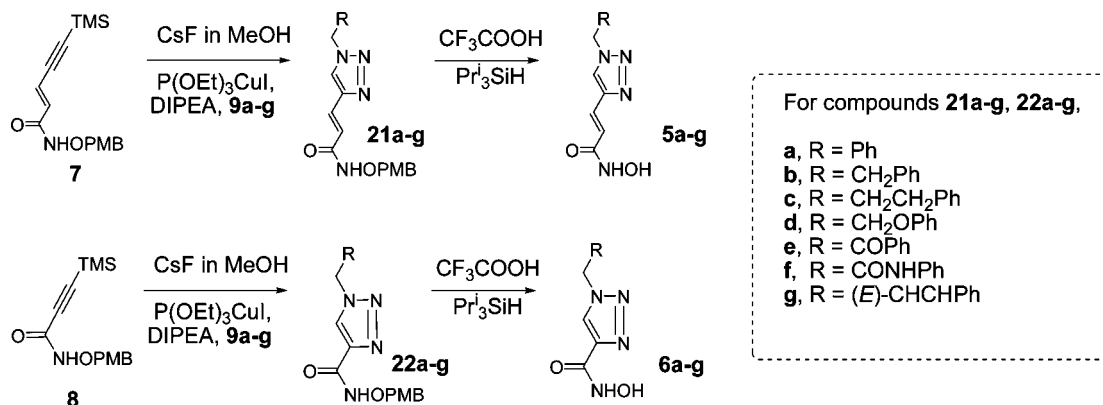
Following preparation of these two libraries, a series of click reactions between alkyne precursors **7** and **8** and the seven azido precursors **9a–g** were performed to afford intermediates **21a–g** and **22a–g** (Scheme 4). In this combinatorial chemistry step, the alkyne precursors were first desilylated with CsF (1 equiv). Following workup, without purification, the crude desilylation intermediates were treated with **9a–g** in the presence of a Cu(I) catalyst to give **21a–g** and **22a–g**. The purified products were then treated with TFA to yield the click HDACi **5a–g** and **6a–g**. These final target compounds were purified by C-18 reverse phase column chromatography due to the presence of an unidentified reddish impurity, which appeared upon addition to normal phase silica gel.

To assess the biological activity of these 14 compounds, they were first tested for inhibition of HDAC. Specifically, HDAC1 and HDAC8 were chosen for the preliminary screen. Selection of these two isozymes stemmed from the previously reported correlation between HDAC1 inhibition and cancer cell growth inhibition,^{40–44} as well as the existence of preferences among several HDAC inhibitors for HDAC1 or HDAC8.^{29,31,45,46} Accordingly, preliminary screening at a concentration of $0.50\text{ }\mu\text{M}$ (Table 1) was conducted. This screening revealed that one of the compounds, **5g**, possessed an inhibitory potency toward HDAC1 that was quite similar to that of SAHA. In addition, several other inhibitors (**5a–5f**, **6a**, **6b**, **6g**) possessed activity against HDAC1, albeit to a lesser extent than either SAHA or **5g**. Of particular importance in this regard is **6g**, given that it showed only $10 \pm 1\%$ inhibition at the concentration tested. This is notable due to the fact that it and **5g**, which demonstrated $75 \pm 5\%$ inhibition, only differ in the length of the linker region. This suggests that a longer linker length considerably aids HDAC1 inhibition in this case.

While the aforementioned 10 compounds showed inhibition against HDAC1, only five of the 14 (**5a**, **6a**, **6b**, **6d**, **6g**) demonstrated any significant inhibition of HDAC8. Of these five, four also possessed activity against HDAC1, with **6d** being the exception. Nonetheless, none of the inhibitors demonstrated as high of a degree of inhibition of HDAC8 as that seen with the inhibition of HDAC1 by SAHA and **5g**.

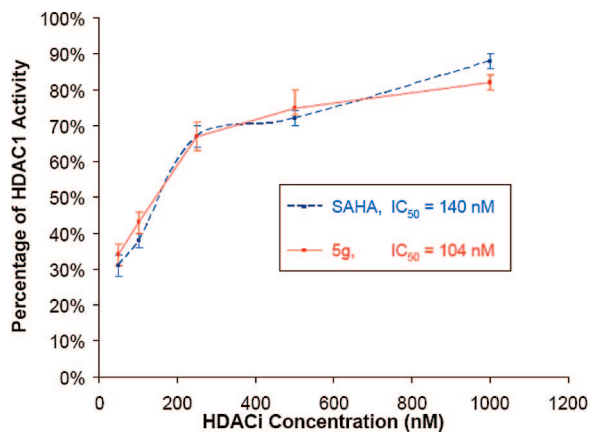
Before better characterizing the activity of these compounds against HDAC (Figure 3), a list of the 14 inhibitors was

Scheme 4. Combinatorial Syntheses of Click HDACi

Table 1. Activity of All HDACi in the Human HDAC1 and HDAC8 Inhibition Tests^a

	SAHA	5a	5b	5c	5d	5e	5f	5g	6a	6b	6c	6d	6e	6f	6g
HDAC 1	72 ± 2	31 ± 4	10 ± 3	8 ± 2	13 ± 4	8 ± 2	15 ± 3	75 ± 5	18 ± 3	9 ± 1	NS	NS	NS	NS	10 ± 1
HDAC 8	NS	12 ± 6	NS	NS	NS	NS	NS	NS	12 ± 2	12 ± 2	NS	26 ± 3	NS	NS	13 ± 2

^a The values given represent the percentage by which the HDAC activity was inhibited by a 0.50 μM HDACi treatment. All of the assays were repeated at least three times. When the inhibition capacity was less than 5%, NS (meaning no significant inhibition) was assigned.

Figure 3. Comparison of HDAC1 inhibition by SAHA and **5g**.

submitted to the National Cancer Institute (NCI) for acceptance into the human cancer cell line screening program, which is provided at no cost. Of the 14, only one, **5g**, ultimately advanced to the final five-dose screen. This selection for advancement stemmed from the results of the single-dose preliminary screen in which the percent inhibition of cell line growth was determined through comparison to untreated samples as described in detail in the Supporting Information. Furthermore, in the five-dose screen (Figure 4), in which data for SAHA is included to serve as a standard, **5g** proved to be active against each of the cancer cell lines in the screen, albeit to varying extents. The differences among the cell lines, however, were generally within or close to 1 order of magnitude. For example, the GI₅₀ values obtained against the various leukemia cell lines all fell within the range of 0.249–2.99 μM. This same trend appeared among the other cancer types for which the ranges were as follows: nonsmall cell lung 0.199–2.26 μM, colon 0.347–2.07 μM, CNS 0.318–1.53 μM, melanoma 0.271–1.08 μM, ovarian 0.187–3.21 μM, renal 0.0100–2.38 μM, prostate 0.580–1.30 μM, and breast 0.180–3.92 μM. As can be seen, the lower end of the range for the renal cancer cell lines is noticeably lower than those of the other cancer types. Specifically, the RXF 393 cell line possessed a GI₅₀ < 10 nM. This represents the lowest GI₅₀ obtained across the 60 cell lines; however, this low value does not appear to be specific to this

type of cancer, but rather cell line specific as the next most sensitive renal cell line (TK-10) possesses a GI₅₀ value of 495 nM.

Given the results of the NCI screen and the fact that **5g** did not show any significant inhibition of HDAC8 at the concentration used in the preliminary screen, a more detailed analysis of HDAC1 inhibition was performed (Figure 3). It was found that **5g** possesses an IC₅₀ value against HDAC1 (104 ± 30 nM) that is comparable to that found with SAHA (140 ± 65 nM). Thus, taken together, the results of the enzyme and cell-based assays provide support to the proposed correlation between the cytotoxicity of HDAC inhibitors and the ability of these agents to inhibit HDAC1. This notion is further supported by the NCI's preliminary cell inhibition studies on the six candidates which were originally selected (Supporting Information). Those compounds which demonstrated a high degree of HDAC1 inhibition (SAHA and **5g**) also exhibited high levels of potency in the cell-based assay. In contrast, the weaker inhibitors of HDAC1 also generally exhibited reduced potency against cancer cells.

Conclusion

This paper highlights the utility of click chemistry in the synthesis of HDACi. Through this approach, a combinatorial strategy was employed that enabled generation of multiple HDACi. Such combinatorial approaches greatly enhance the efficiency of drug discovery as libraries of candidate molecules can be obtained rapidly. This fact was highlighted by the discovery of lead compound **5g**, which was found to inhibit HDAC1 with an IC₅₀ = 104 ± 30 nM while demonstrating no significant inhibition of HDAC8 in preliminary testing. This level of inhibition was found to be comparable to that exhibited by the clinically approved drug SAHA (140 ± 65 nM). Furthermore, **5g** was also found to be active across all cell lines in the NCI human cancer cell line screen, with GI₅₀ values ranging from 3.92 μM to 10 nM.

In summary, we have developed a click chemistry approach to HDACi design, which has not only led to a potent lead compound, but more importantly, one which is readily amenable to further derivatization. For example, functionalization of the aromatic ring, replacement of the aromatic ring with a heteroaromatic species, or introduction of a chiral center in the

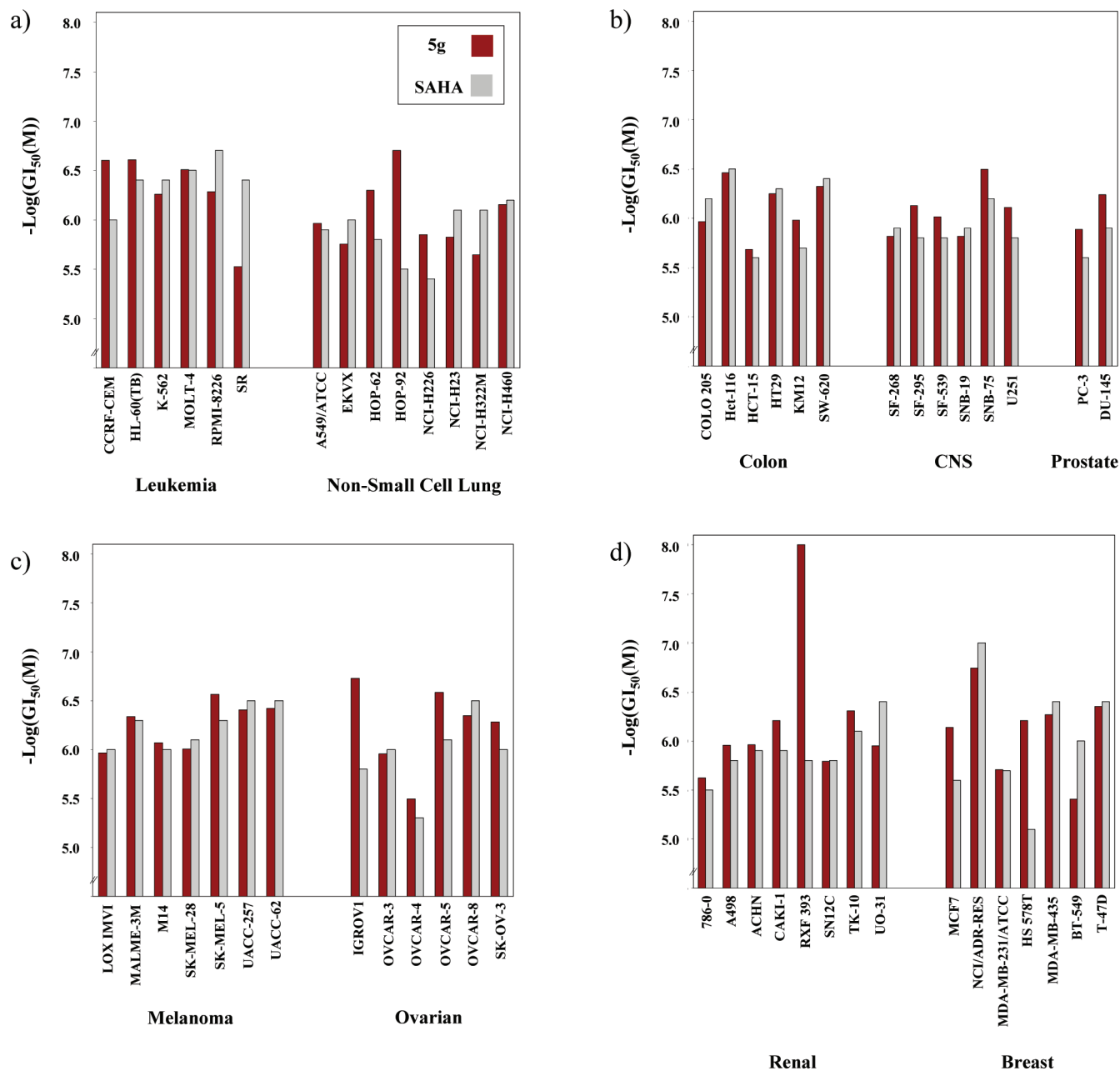


Figure 4. Comparison of GI₅₀ values from the NCI human cancer cell line screen for **5g** and SAHA. Tested doses included 1×10^{-4} , 1×10^{-5} , 1×10^{-6} , 1×10^{-7} , and 1×10^{-8} M. (a) Activity against leukemia and nonsmall cell lung cancer cell lines. (b) Activity against colon, central nervous system (CNS) and prostate cancer cell lines. (c) Activity against melanoma and ovarian cancer cell lines. (d) Activity against renal and breast cancer cell lines.

“cap” moiety can all occur quite readily by incorporating these features into the azide-containing fragment. This will allow modifications to occur prior to the combinatorial step, thus maintaining the modular nature of this approach. A large number of new candidate molecules can therefore be rapidly prepared via modification of the azide library.

Experimental Section

All solvents were dried with a solvent-purification system from Innovative Technology, Inc. All reagents were obtained from commercial sources and used without further purification. Analytical TLC was carried out on silica gel 60 F254 aluminum-backed plates (E. Merck). The 230–400 mesh size of the same absorbent was utilized for all chromatographic purifications. The 200–400 mesh silica gel 60 RP-18 (from EMD) was utilized to purify the target click HDACi. ¹H and ¹³C NMR spectra were recorded at the

indicated field strengths. The high-resolution mass spectra were collected at The Ohio State University Campus Chemical Instrumentation Center. The purities of click HDACi were analyzed by HPLC (refer to the Supporting Information). The purity of the key target compound **5g** is 98.3%, with the purities of the other 13 target compounds all being higher than 96%. As for the HDAC1 and HDAC8 inhibition studies, the assay kits were obtained from Biomol International LP. All assays were repeated at least three times. Briefly, the assay was performed in two stages. In the first stage, HDAC8 solution (15 μ L, 1 U total), HDACi solution (10 μ L), and HDAC8 substrate solution (25 μ L) were added to the 96-well microplate. The reaction proceeded at 30 °C for 45 min. The second stage was initiated by the addition of 50 μ L of developer, which stopped HDAC activity and produced the fluorescent signal ($\lambda_{\text{ex}} = 350$ nm; $\lambda_{\text{em}} = 450$ nm). The cell line assays for the selected six target compounds, **5b** (NSC746454), **5e** (NSC746455), **5f** (NSC746456), **5g** (NSC746457), **6e** (NSC746458), and **6g**

(NSC746459), were performed by the NIH.⁴⁷ Cell lines tested consisted of the following: CCRF-CEM, HL-60(TB), K-562, MOLT-4, RPMI-8226, and SR (leukemia); A549/ATCC, EKVX, HOP-62, HOP-92, NCI-H226, NCI-H23, NCI-H322 M, and NCI-H460 (non-small cell lung cancer); COLO 205, HCT-116, HCT-15, HT29, KM12, and SW-620 (colon cancer); SF-628, SF-295, SF-539, SNB-19, SNB-75, and U251 (CNS cancer); LOX IMVI, MALME-3M, M14, SK-MEL-28, SK-MEL-5, UACC-257, and UACC-62 (melanoma); IGROV1, OVCAR-3, OVCAR-4, OVCAR-5, OVCAR-8, and SK-OV-3 (ovarian cancer); 786-0, A498, ACHN, CAKI-1, RXF 393, SN12C, TK-10, and UO-31 (renal cancer); PC-3 and DU-145 (prostate cancer); MCF7, NCI/ADR-RES, MDA-MB-231/ATCC, HS578T, MDA-MB-435, BT-549, and T-47D (breast cancer). Full experimental details are available free of charge via the Internet at <http://dtp.nci.nih.gov/branches/btb/ivclsp.html>.^{48,49}

General Procedure for the Preparation of Click HDACi 5a–g and 6a–g from 21a–g and 22a–g. Triisopropylsilane (3 mmol, 0.6 mL, 3 equiv), PMB protected substrate (**21a–g** or **22a–g**, 1 mmol, 1.0 equiv), and TFA (2 mL) were added in sequence to a reaction vessel containing DCM (40 mL). The mixture was stirred at room temperature and monitored by TLC. Upon completion, the reaction mixture was diluted with acetonitrile (100 mL) and then neutralized with DOWEX Marathon WBA anion exchange resin (from Aldrich). The resin was washed additionally with acetonitrile (50 mL × 2). The combined organic solution was evaporated to provide a solid, which was purified to afford the final product.

(E)-3-(1-Benzyl-1H-1,2,3-triazol-4-yl)-N-hydroxyacrylamide (5a). The crude product was first dissolved with a minimal amount of 5% methanol in DCM, after which the pure compound was precipitated with hexanes (4× the original volume) as a slightly pink solid (28 mg **5a** from 100 mg **21a**, 42% yield). ¹H NMR (500 MHz, CD₃OD): δ 8.15 (s, 1H), 7.50 (d, *J* = 15.8 Hz, 1H), 7.42–7.28 (m, 5H), 6.62 (d, *J* = 15.8 Hz, 1H), 5.60 (s, 2H). ¹³C NMR (125 MHz, CD₃OD): δ 165.8, 145.2, 136.7, 130.2, 129.8, 129.3, 125.7, 120.4, 55.1 (one peak less due to overlap ~130). HRMS (ESI) calcd for C₁₂H₁₂N₄O₂Na [M + Na]⁺ 267.0858, found 267.0860.

(E)-N-Hydroxy-3-(1-phenethyl-1H-1,2,3-triazol-4-yl)acrylamide (5b). The crude product was purified via C-18 reverse phase column chromatography (water:acetonitrile = 5:1) to provide **5b** as a white solid (65 mg **5b** from 174 mg **21b**, 55% yield). ¹H NMR (500 MHz, DMF-*d*₇): δ 8.32 (s, 1H), 7.48 (d, *J* = 15.7 Hz, 1H), 7.36–7.20 (m, 5H), 6.74 (d, *J* = 15.7 Hz, 1H), 4.73 (t, *J* = 7.3 Hz, 2H), 3.27 (t, *J* = 7.3 Hz, 2H). ¹³C NMR (125 MHz, CD₃OD): δ 163.9, 144.4, 139.0, 129.9, 129.6, 128.5, 127.8, 125.5, 120.6, 52.0, 37.1. HRMS (ESI) calcd for C₁₃H₁₄N₄O₂Na [M + Na]⁺ 281.1014, found 281.1017.

(E)-N-Hydroxy-3-(1-(3-phenylpropyl)-1H-1,2,3-triazol-4-yl)acrylamide (5c). The crude product was purified via C-18 reverse phase column chromatography (water:acetonitrile = 5:1) to provide a pale-colored solid (35 mg product **5c** from 100 mg **21c**, 50% yield). ¹H NMR (500 MHz, CD₃OD): δ 8.15 (s, 1H), 7.51 (d, *J* = 15.8 Hz, 1H), 7.30–7.24 (m, 2H), 7.21–7.15 (m, 3H), 6.62 (d, *J* = 15.8 Hz, 1H), 4.42 (t, *J* = 7.2 Hz, 2H), 2.64 (t, *J* = 7.5 Hz, 2H), 2.41 (tt, *J*₁ = *J*₂ = 7.4 Hz, 2H). ¹³C NMR (125 MHz, CD₃OD): δ 165.9, 144.9, 142.0, 129.7, 129.6, 129.4, 127.4, 125.8, 120.2, 51.0, 33.6, 33.0. HRMS (ESI) calcd for C₁₄H₁₆N₄O₂Na [M + Na]⁺ 295.1171, found 295.1168.

(E)-N-Hydroxy-3-(1-(2-phenoxyethyl)-1H-1,2,3-triazol-4-yl)acrylamide (5d). The crude product was purified via C-18 reverse phase column chromatography (water:acetonitrile = 6:1) to provide a white solid (69 mg **5d** from 163 mg **21d**, 61% yield). ¹H NMR (500 MHz, DMF-*d*₇): δ 8.52 (s, 1H), 7.52 (d, *J* = 15.8 Hz, 1H), 7.38–7.24 (m, 2H), 7.07–6.92 (m, 3H), 6.79 (d, *J* = 15.7 Hz, 1H), 4.91 (t, *J* = 5.0 Hz, 2H), 4.51 (t, *J* = 5.0 Hz, 2H). ¹³C NMR (125 MHz, DMF-*d*₇): δ 163.8, 159.3, 144.7, 130.6, 128.3, 126.0, 122.2, 120.8, 115.7, 67.3 50.6. HRMS (ESI) calcd for C₁₃H₁₄N₄O₃Na [M + Na]⁺ 297.0964, found 297.0966.

(E)-N-Hydroxy-3-(1-(2-oxo-2-phenylethyl)-1H-1,2,3-triazol-4-yl)acrylamide (5e). The crude product was purified via C-18 reverse phase column chromatography (water:acetonitrile = 6:1) to provide a pale-colored solid (22 mg product **5e** from 90 mg **21e**, 35%). ¹H NMR (500 MHz, DMF-*d*₇): δ 11.19 (s, 1H), 8.48 (s, 1H), 8.17 (d, *J* = 7.4 Hz, 2H), 7.80 (t, *J* = 7.9 Hz, 1H), 7.67 (dd, *J*₁ = *J*₂ = 7.8 Hz, 2H), 7.62 (d, *J* = 15.2 Hz, 1H), 6.85 (d, *J* = 15.7 Hz, 1H), 6.34 (s, 2H). ¹³C NMR (125 MHz, DMF-*d*₇): δ 192.2, 143.6, 134.4, 134.4, 129.2, 128.3, 127.7, 126.4, 119.8, 56.1 (one peak less due to the overlap with solvent peak ~ δ 162). HRMS (ESI) calcd for C₁₃H₁₂N₄O₃Na [M + Na]⁺ 295.0807, found 295.0811.

(E)-N-Hydroxy-3-(1-(2-oxo-2-(phenylamino)ethyl)-1H-1,2,3-triazol-4-yl)acrylamide (5f). The crude product was purified via C-18 reverse phase column chromatography (water:acetonitrile:TFA = 6:1:0.03) to provide a pink solid (67 mg **5f** from 187 mg **21f**, 71% yield). ¹H NMR (500 MHz, DMF-*d*₇): δ 10.60 (s, 1H), 8.49 (s, 1H), 7.69 (d, *J* = 7.5 Hz, 2H), 7.57 (d, *J* = 15.7 Hz, 1H), 7.36 (apparent t, *J* = 7.4 Hz, 2H), 7.12 (t, *J* = 7.4 Hz, 1H), 6.81 (d, *J* = 15.7 Hz, 1H), 5.51 (s, 2H). ¹³C NMR (125 MHz, CD₃OD): δ 165.4, 144.5, 140.0, 129.9, 128.5, 127.2, 124.9, 120.8, 120.4, 53.6. HRMS (ESI) calcd for C₁₃H₁₃N₅O₃Na [M + Na]⁺ 310.0916, found 310.0923.

(E)-3-(1-Cinnamyl-1H-1,2,3-triazol-4-yl)-N-hydroxyacrylamide (5g). The crude product was purified via C-18 reverse phase column chromatography (water:acetonitrile = 5:1) to provide a white solid (96 mg **5g** from 199 mg **21g**, 70% yield). ¹H NMR (500 MHz, DMF-*d*₇): δ 10.2 (br s, 1H), 8.48 (s, 1H), 7.58–7.48 (m, 3H), 7.37 (apparent t, *J* = 7.4 Hz, 2H), 7.30 (t, *J* = 7.1 Hz, 1H), 6.82 (d, *J* = 16.0 Hz, 1H), 6.77 (d, *J* = 15.8 Hz, 1H), 6.60 (dt, *J*₁ = 15.5 Hz, *J*₂ = 6.2 Hz, 1H), 5.29 (d, *J* = 6.1 Hz, 2H). ¹³C NMR (125 MHz, DMF-*d*₇): δ 163.9, 144.9, 137.2, 129.7, 135.3, 129.2, 128.3, 127.8, 125.3, 124.5, 120.9, 52.8. HRMS (ESI) calcd for C₁₄H₁₄N₄O₂Na [M + Na]⁺ 293.1014, found 293.1020.

1-Benzyl-1H-[1,2,3]triazole-4-carboxylic Acid Hydroxamide (6a). The crude product was purified via C-18 reverse phase column chromatography (water:acetonitrile = 6:1) to provide a white solid (16 mg **6a** from 53 mg **22a**, 47% yield). ¹H NMR (500 MHz, DMF-*d*₇): δ 11.40–9.20 (bd s, 1H), 8.64 (s, 1H), 7.58–7.28 (m, 5H), 5.76 (s, 2H). ¹³C NMR (125 MHz, DMF-*d*₇): δ 158.9, 143.1, 137.0, 129.9, 129.3, 129.1, 127.1, 54.4. HRMS (ESI) calcd for C₁₀H₁₀N₄O₂Na [M + Na]⁺ 241.0701, found 241.0697.

1-Phenethyl-1H-[1,2,3]triazole-4-carboxylic Acid Hydroxamide (6b). The crude product was purified via C-18 reverse phase column chromatography (water:acetonitrile = 6:1) to provide a white solid (21 mg **6b** from 63 mg **22b**, 51% yield). ¹H NMR (500 MHz, DMF-*d*₇): δ 11.21 (s, 1H), 9.30 (s, 1H), 8.48 (s, 1H), 7.40–7.20 (m, 5H), 4.78 (t, *J* = 7.3 Hz, 2H), 3.29 (t, *J* = 7.3 Hz, 2H). ¹³C NMR (125 MHz, DMF-*d*₇): δ 158.3, 141.9, 138.0, 129.0, 128.7, 126.9, 126.2, 51.3, 36.2. HRMS (ESI) calcd for C₁₁H₁₂N₄O₂Na [M + Na]⁺ 255.0858, found 255.0862.

1-(3-Phenyl-propyl)-1H-[1,2,3]triazole-4-carboxylic Acid Hydroxamide (6c). The crude product was purified via C-18 reverse phase column chromatography (water:acetonitrile = 6:1) to provide a white solid (31 mg **6c** from 63 mg **22c**, 74% yield). ¹H NMR (500 MHz, DMF-*d*₇): δ 11.27 (s, 1H), 9.38 (s, 1H), 8.61 (s, 1H), 7.36–7.20 (m, 5H), 4.54 (t, *J* = 7.1 Hz, 2H), 2.66 (t, *J* = 7.7 Hz, 2H), 2.26 (tt, *J*₁ = *J*₂ = 7.1 Hz, 2H). ¹³C NMR (125 MHz, DMF-*d*₇): δ 159.1, 142.8, 142.0, 129.4, 127.0, 126.9, 55.7, 50.5, 33.2, 32.7. HRMS (ESI) calcd for C₁₂H₁₄N₄O₂Na [M + Na]⁺ 269.1014, found 269.1014.

1-(2-Phenoxy-ethyl)-1H-[1,2,3]triazole-4-carboxylic Acid Hydroxamide (6d). The crude product was purified via C-18 reverse phase column chromatography (water:acetonitrile = 6:1) to provide a white solid (15 mg **6d** from 40 mg **22d**, 56% yield). ¹H NMR (500 MHz, DMF-*d*₇): δ 10.60–9.90 (bd s, 1H), 8.65 (s, 1H), 7.34–7.28 (m, 2H), 7.00–6.94 (m, 2H), 4.95 (t, *J* = 5.1 Hz, 2H), 4.53 (t, *J* = 5.1 Hz, 2H). ¹³C NMR (125 MHz, DMF-*d*₇): δ 159.4, 159.1, 143.0, 130.6, 127.6, 122.2, 115.7, 67.3, 50.7. HRMS (ESI) calcd for C₁₁H₁₂N₄O₂Na [M + Na]⁺ 271.0807, found 271.0807.

1-(2-oxo-2-Phenyl-ethyl)-1H-[1,2,3]triazole-4-carboxylic Acid Hydroxyamide (6e). The crude product was purified via C-18 reverse phase column chromatography (water:acetonitrile = 7:1) to provide a white solid (56 mg **6e** from 116 mg **22e**, 72% yield). ¹H NMR (500 MHz, DMF-*d*₇): δ 11.40–9.20 (bd s, 2H), 8.62 (s, 1H), 8.16 (d, *J* = 7.3 Hz, 2H), 7.78 (t, *J* = 7.4 Hz, 1H), 7.65 (dd, *J*₁ = *J*₂ = 7.8 Hz, 2H), 6.38 (s, 2H). ¹³C NMR (125 MHz, DMF-*d*₇): δ 192.9, 159.1, 143.0, 135.5, 135.3, 130.1, 129.3, 128.9, 57.3. HRMS (ESI) calcd for C₁₁H₁₀N₄O₃Na [M + Na]⁺ 269.0651, found 269.0629.

1-Phenylcarbamoylmethyl-1H-[1,2,3]triazole-4-carboxylic Acid Hydroxyamide (6f). The crude product was purified via C-18 reverse phase column chromatography (water:acetonitrile = 7:1) to provide a white solid (45 mg **6f** from 120 mg **22f**, 55% yield). ¹H NMR (500 MHz, DMF-*d*₇): δ 10.77 (s, 1H), 10.50–10.00 (bd s, 1H), 8.65 (s, 1H), 7.70 (d, *J* = 7.4 Hz, 2H), 7.35 (dd, *J*₁ = *J*₂ = 7.9 Hz, 2H), 7.11 (t, *J* = 7.4 Hz, 1H), 5.57 (s, 2H). ¹³C NMR (125 MHz, DMF-*d*₇): δ 165.3, 159.1, 142.8, 140.1, 129.9, 128.8, 124.8, 120.4, 53.6. HRMS (ESI) calcd for C₁₁H₁₁N₅O₃Na [M + Na]⁺ 284.0760, found 284.0743.

1-(3-Phenyl-allyl)-1H-[1,2,3]triazole-4-carboxylic Acid Hydroxyamide (6g). The crude product was purified via C-18 reverse phase column chromatography (water:acetonitrile = 5:1) to provide a white solid (21 mg **6g** from 62 mg **22g**, 50% yield). ¹H NMR (500 MHz, DMF-*d*₇): δ 10.60–9.80 (bd s, 2H), 8.61 (s, 1H), 7.53 (d, *J* = 7.6 Hz, 2H), 7.38 (dd, *J*₁ = *J*₂ = 7.5 Hz, 2H), 7.31 (t, *J* = 7.3 Hz, 1H), 6.79 (d, *J* = 15.9 Hz, 1H), 6.62 (td, *J*₁ = 15.7 Hz, *J*₂ = 6.6 Hz, 1H), 5.33 (d, *J* = 6.5 Hz, 2H). ¹³C NMR (125 MHz, DMF-*d*₇): δ 159.4, 159.1, 143.0, 130.6, 127.6, 122.2, 115.7, 67.3, 50.7. HRMS (ESI) calcd for C₁₂H₁₂N₄O₂Na [M + Na]⁺ 267.0858, found 267.0855.

(E)-N-(4-Methoxybenzyloxy)-5-(trimethylsilyl)pent-2-en-4-ynamide (7). The acid **19** (168 mg, 1.0 mmol, 1.0 equiv) was added to a reaction vessel containing DCM (3 mL). To this solution, oxalyl chloride (130 μL, 1.6 mmol, 1.6 equiv) and a trace amount of DMF were added. The mixture was stirred at room temperature for 1 h. The solvent was then removed under vacuum to afford a yellow–reddish syrup. DCM (4 mL) was added, and the flask was cooled to 0 °C (solution A). The amine **13** (285 mg 1.5 mmol, 1.5 equiv) and *N,N*-diisopropylethylamine (DIPEA) (0.52 mL, 3.0 mmol, 3.0 equiv) were added to a second reaction vessel containing DCM (10 mL) (solution B). Solution B was cooled to 0 °C, after which solution A was added within 1 min. The mixture was stirred for one-half hour at 0 °C. The reaction mixture was then poured into ice-cold 0.1 N HCl (20 mL), after which DCM (20 mL) was added. The organic layer was additionally washed with ice-cold 0.1 N HCl (2 × 20 mL). The DCM solution was dried with Na₂SO₄, and the solvent was evaporated. The crude product was purified via flash column chromatography (hexanes:ethyl acetate, 87:13 to 83:17) to provide pure **7** as a white oil (253 mg, 84%). ¹H NMR (500 MHz, CD₃CN): δ 9.44 (bd s, 1H), 7.33 (d, *J* = 8.6 Hz, 2H), 6.92 (d, *J* = 8.6 Hz, 2H), 6.64 (d, *J* = 15.5 Hz, 1H), 6.17 (d, *J* = 14.2 Hz, 1H), 4.79 (s, 2H), 3.79 (s, 3H), 0.20 (s, 9H). ¹³C NMR (125 MHz, CD₃CN): δ 163.0, 161.0, 132.3, 132.0, 128.7, 121.4, 114.8, 103.2, 102.8, 78.4, 55.9, –0.33. HRMS (ESI) calcd for C₁₆H₂₁NO₃SiNa [M + Na]⁺ 326.1188, found 326.1193.

(E)-N-(4-Methoxybenzyloxy)-5-(trimethylsilyl)-N-(E)-5-(trimethylsilyl)pent-2-en-4-ynoyl)pent-2-en-4-ynamide (20). Compound **20** was a byproduct obtained during the preparation of **7**. ¹H NMR (500 MHz, CD₃CN): δ 7.25 (d, *J* = 8.6 Hz, 2H), 6.90 (d, *J* = 8.7 Hz, 2H), 6.88 (d, *J* = 15.9 Hz, 1H), 6.48 (d, *J* = 16.0 Hz, 1H), 6.34 (d, *J* = 15.9 Hz, 1H), 6.12 (d, *J* = 16.0 Hz, 1H), 5.00 (s, 1H), 3.78 (s, 1H), 0.22 (s, 9H), 0.18 (s, 9H). ¹³C NMR (125 MHz, CD₃CN): δ 161.3, 160.8, 149.0, 131.1, 131.0, 129.7, 129.6, 128.8, 116.4, 114.8, 108.2, 103.1, 103.1, 101.6, 77.8, 55.9, –0.30, –0.51. HRMS (ESI) calcd for C₂₄H₃₁NO₄Si₂Na [M + Na]⁺ 476.1689, found 476.1683.

N-(4-Methoxybenzyloxy)-3-(trimethylsilyl)propiolamide (8). Commercially available acid **14** (710 mg, 5.0 mmol, 1.0 equiv) was added to a reaction vessel containing DCM (10 mL). To this solution, oxalyl chloride (430 μL, 5.5 mmol, 1.1 equiv) and a trace

amount of DMF were added. The mixture was stirred at room temperature for 2 h. The solution was then placed in an ice bath, and most of the acidic gases (HCl and SO₂) were removed under vacuum (~20 bar) to give a yellow solution. Freshly dried DCM (10 mL) was then added (solution A). The amine **13** (950 mg, 5.0 mmol, 1.0 equiv) and DIPEA (2.8 mL, 16.1 mmol, 3.2 equiv) were added to a second reaction vessel containing DCM (50 mL) (solution B). Solution B was cooled to 0 °C, after which solution A was added within 1 min. The mixture was then stirred for 30 min at 0 °C. The reaction mixture was poured onto ice-cold 0.1 N HCl (200 mL) before DCM (200 mL) was also added. The organic layer was additionally washed with ice-cold 0.1 N HCl twice (2 × 100 mL). The DCM solution was dried with Na₂SO₄, and the solvent was evaporated. The crude product was purified via flash column chromatography (hexanes:ethyl acetate, 85:15 to 80:20) to provide **8** as pale-colored oil (0.85 g, 61%). ¹H NMR (500 MHz, CDCl₃): δ 8.43 (bd s, 1H), 7.32 (d, *J* = 8.5 Hz, 2H), 6.89 (dd, *J* = 8.5 Hz, 2H), 4.85 (s, 2H), 3.80 (s, 3H), 0.20 (s, 9H). ¹³C NMR (125 MHz, CDCl₃): δ 160.1, 151.0, 131.0, 126.9, 114.0, 95.0, 94.4, 78.2, 55.3, 0.8. HRMS (ESI) calcd for C₁₄H₁₉NO₃SiNa [M + Na]⁺ 300.1032, found 300.1033.

General Procedure to Prepare the Azido Precursors 9a–g. An alkyl halide **10a–g** (1.5 g, 1.0 equiv) was added to a reaction vessel containing a solution of NaN₃ in DMSO (1.1 equiv, 0.5 M). The reaction was monitored by NMR analysis. Upon completion of the reaction, water (50 mL) was added and the product was extracted with ether (3 × 50 mL). The combined organic layers were washed with water (2 × 50 mL) and brine (50 mL) and dried with magnesium sulfate. The organic solvent was removed to provide the azido compound. For **9c** and **9d**, a catalytic amount of tetraethylammonium bromide (0.05 mol%, 0.005 equiv) was added. The spectral data were in agreement with those reported.^{36,50–53}

(Azidomethyl)benzene (9a). From **10a** (1.5 g, 11.3 mmol, 1.0 equiv), **9a** was obtained in 95% yield as a colorless liquid. ¹H NMR (500 MHz, CDCl₃): δ 7.75–7.40 (m, 5H), 4.35 (s, 2H).³⁶

(2-Azidoethyl)benzene (9b). From **10b** (1.5 g, 10.2 mmol, 1.0 equiv), **9b** was obtained in 93% yield as a colorless liquid. ¹H NMR (500 MHz, CDCl₃): δ 7.33 (t, *J* = 7.2 Hz, 2H), 7.26 (d, *J* = 7.1 Hz, 1H), 7.23 (d, *J* = 7.2 Hz, 2H), 3.51 (t, *J* = 7.3 Hz, 2H), 2.91 (t, *J* = 7.3 Hz, 2H).^{50,51}

(3-Azidopropyl)benzene (9c). From **10c** (1.5 g, 9.30 mmol, 1.0 equiv), **9c** was obtained in 90% yield as a colorless liquid. ¹H NMR (500 MHz, CDCl₃): δ 7.30 (t, *J* = 7.3 Hz, 2H), 7.24–7.16 (m, 3H), 3.29 (t, *J* = 7.3 Hz, 2H), 2.71 (t, *J* = 7.6 Hz, 2H), 1.92 (tt, *J*₁ = *J*₂ = 7.2 Hz, 2H).^{50,51}

(2-Azidoethoxy)benzene (9d). From **10d** (1.5 g, 9.2 mmol, 1.0 equiv), **9d** was obtained in 95% yield as a colorless liquid. ¹H NMR (500 MHz, CDCl₃): δ 7.34–7.28 (m, 2H), 7.02–6.97 (m, 1H), 6.95–6.89 (m, 2H), 4.16 (d, *J* = 5.0 Hz, 2H), 3.60 (d, *J* = 5.0 Hz, 2H). ¹³C NMR (125 MHz, CDCl₃): δ 158.4, 129.8, 121.6, 114.8, 67.1, 50.4.

2-Azido-1-phenylethanone (9e). From **10e** (1.5 g, 8.0 mmol, 1.0 equiv), **9e** was obtained in 75% yield after flash column chromatography (2–5% ether in hexanes) as a colorless liquid. ¹H NMR (500 MHz, CDCl₃): δ 7.91–7.88 (m, 2H), 7.65–7.60 (m, 1H), 7.53–7.48 (m, 2H), 4.56 (s, 2H).⁵²

2-Azido-N-phenylacetamide (9f). From **10f** (1.5 g, 8.5 mmol, 1.0 equiv), **9f** was obtained in 90% yield as a colorless liquid. ¹H NMR (500 MHz, CDCl₃): δ 8.00 (bd s, 1H), 7.54 (d, *J* = 8.6 Hz, 2H), 7.35 (dd, *J*₁ = 8.4 Hz, *J*₂ = 7.5 Hz, 2H), 7.16 (d, *J* = 8.6 Hz, 1H), 4.15 (s, 2H).⁵³

2-Azido-N-phenylacetamide (9g). From **10g** (1.5 g, 9.4 mmol, 1.0 equiv), **9g** was obtained in 87% yield as a colorless liquid. ¹H NMR (500 MHz, DMSO-*d*₆): δ 7.51–7.47 (m, 2H), 7.38–7.31 (m, 2H), 7.31–7.26 (m, 1H), 6.71 (d, *J* = 15.8 Hz, 1H), 6.39 (dt, *J*₁ = 15.8 Hz, *J*₂ = 6.6 Hz, 1H), 4.04 (d, *J* = 6.6 Hz, 2H).³⁶

O-(4-Methoxybenzyl)hydroxylammonium Chloride (13). *N*-Hydroxyphthalimide **11** (4.9 g, 30 mmol, 1.0 equiv) and potassium carbonate (5.0 g, 36 mmol, 1.2 equiv) were added to a reaction vessel containing DMF (100 mL). To this solution, 1-(chloromethyl)-4-methoxybenzene (PMBCl) (4.7 mL, 33 mmol, 1.1 equiv)

was added. The reaction continued overnight at room temperature. Water (500 mL) and benzene (500 mL) were then added. The aqueous layer was additionally extracted with benzene (2 × 100 mL). The combined organic layers were washed with sat. NaHCO₃ solution (3 × 200 mL) and dried with magnesium sulfate. Crude **12** was obtained after removal of the solvent and was directly employed in the next step. To this crude product in methanol (500 mL), hydrazine monohydrate was added (4.5 mL, 92.5 mmol, 3.1 equiv). The mixture was stirred overnight at room temperature. TLC analysis indicated the presence of a new compound. Upon completion of the reaction, the solution pH was adjusted to 2 via the addition of aqueous 2 M HCl. The mixture was cooled in an ice bath for 1 h, after which the white precipitate (byproduct) was removed. The solvent was removed, and the residue/syrup was partitioned between DCM (200 mL) and ammonium bicarbonate solution (pH = 8, 200 mL). The organic layer was dried with Na₂SO₄. Addition of 1 M HCl in ether then caused the product **13** to precipitate as a white solid (4.3 g, 75.6% yield for two steps). Spectral data were in agreement with those reported.³⁷ ¹H NMR (500 MHz, DMSO-*d*₆): δ 11.10 (bd s, 3H), 7.35 (d, *J* = 8.6 Hz, 2H), 6.96 (d, *J* = 8.6 Hz, 2H), 4.97 (s, 2H), 3.76 (s, 3H).

(E)-3-Iodopropenoic acid (16). Propiolic acid **15** (10 mL, 162.0 mmol, 1.0 equiv) was added over 1 min to a reaction vessel containing a solution of CuI (200 mg, 1.1 mmol, 0.007 equiv) and HI (40 mL, initially 57%, 303.2 mmol, 1.9 equiv). The reaction mixture was immediately immersed in a preheated oil bath (130 °C) for 30 min. The reaction was then cooled to room temperature over a 15 min period. A white precipitate formed, after which the solution was kept at room temperature for another 15 min. The liquid was removed by filtration, and the solid was washed with water (3 × 70 mL). Following a period of drying, the pure iodoacid **16** was obtained as white needles (23.9 g, 75%). ¹H NMR (500 MHz, CDCl₃): δ 10.54–8.66 (bd s, 1H), 8.07 (d, *J* = 14.9 Hz, 1H), 6.88 (d, *J* = 14.9 Hz, 1H). Spectral data were in agreement with those reported.³⁸

(2-Methoxyethoxy)methyl-(2E)-3-iodoprop-2-enoate (17). K₂CO₃ (3.42 g, 24.8 mmol, 1.2 equiv) and 2-methoxyethoxymethyl chloride (MEMCl) (3.2 mL, 27.6 mmol, 1.3 equiv) were added to a reaction vessel containing a solution of *E*-iodopropenoic acid **16** (4.2 g, 21.2 mmol, 1.0 equiv) in DMF (20 mL). The mixture was stirred at ambient temperature for 1 h, poured onto water (20 mL), and then extracted with ether (3 × 20 mL). The combined organic layers were washed with water, brine, dried over MgSO₄, and concentrated. Flash column chromatography (hexanes:ethyl acetate, 20:1 to 10:1) provided 5.2 g (86%) of **17** as a colorless oil. ¹H NMR (500 MHz, C₆D₆): δ 7.62 (d, *J* = 14.8 Hz, 1H) 6.62 (d, *J* = 14.8 Hz, 1H), 5.13 (s, 2H), 3.49 (t, *J* = 4.7 Hz, 2H), 3.18 (t, *J* = 4.7 Hz, 2H), 3.04 (s, 3H). ¹³C NMR (125 MHz, C₆D₆): δ 163.1, 136.6, 100.2, 89.9, 71.8, 69.9, 58.7. HRMS (ESI) calcd for C₇H₁₁O₄Na [M + Na]⁺ 308.9600, found 308.9605.

(2-Methoxyethoxy)methyl-(2E)-5-(trimethylsilyl)pent-2-en-4-ynoate (18). Pd(PPh₃)₂Cl₂ (0.56 g, 0.80 mmol, 0.8 equiv) and CuI (0.31 g, 1.63 mmol, 0.1 equiv) were added to a reaction vessel containing a solution of the iodide **17** (4.65 g, 16.3 mmol, 1.0 equiv) in Et₃N (60 mL). The solution was degassed with argon. Trimethylsilylacetylene (3.8 mL, 29.3 mmol, 1.8 equiv) was then added and the solution was stirred for 1 h. The mixture was poured into sat. NH₄Cl (200 mL) and extracted with ether (3 × 100 mL). The combined organic layers were washed with brine, dried over MgSO₄, and concentrated. The thick oily residue was subjected to flash column chromatography (hexanes:ethyl acetate, 20:1 to 13:1) to yield 3.6 g (87%) of **18** as a pale oil. ¹H NMR (500 MHz, CDCl₃): δ 6.77 (d, *J* = 16.0 Hz, 1H), 6.23 (d, *J* = 16.0 Hz, 1H), 5.38 (s, 2H), 3.77 (m, 2H), 3.53 (m, 2H), 3.36 (s, 3H), 0.20 (s, 9H). ¹³C NMR (125 MHz, CDCl₃): δ 165.1, 130.6, 126.0, 105.9, 101.1, 89.8, 71.5, 69.6, 59.1, -0.43. HRMS (ESI) calcd for C₁₂H₂₀O₄SiNa [M + Na]⁺ 279.1029, found 279.1032.

(E)-5-(Trimethylsilyl)pent-2-en-4-ynoic acid (19). MEM-protected **18** (3.07 g, 12.0 mmol, 1.0 equiv) and 3N HCl (12 mL) were added to a reaction vessel containing THF (150 mL). The reaction was stirred at room temperature for 3 days, during which

time it was monitored by TLC (5% MeOH in dichloromethane, *R*_f = 0.10). The solution was then concentrated and the residue partitioned between water (250 mL) and CH₂Cl₂ (100 mL). The water was further extracted with CH₂Cl₂ (2 × 100 mL). The combined organic layers were washed with brine, dried over MgSO₄, and concentrated to give 2.01 g (~100%) of the crude acid **19** as pale-yellow solid. The crude product was pure enough for NMR analysis. ¹H NMR (500 MHz, CDCl₃): δ 0.20 (s, 9H), 6.22 (d, *J* = 15.9 Hz, 1H), 6.80 (d, *J* = 15.9 Hz, 1H), 12.5–11.0 (bd s, 1H). ¹³C NMR (125 MHz, CDCl₃): δ -0.34, 101.1, 107.1, 127.6, 130.4, 171.4. HRMS (ESI) calcd for C₈H₁₂O₂SiNa [M + Na]⁺ 191.0502, found 191.0504.

General Procedure for the Preparation of 21a–g. The alkyne precursor **7** (152 mg, 0.5 mmol, 1.0 equiv) was added to a reaction vessel containing THF (5 mL) and MeOH (5 mL). Cesium fluoride (91 mg, 0.6 mmol, 1.2 equiv) was then added, after which the reaction was monitored by TLC analysis. The desilylation intermediate was slightly more polar than the reactant. Upon disappearance of the reactant, the solvent was removed, followed by partitioning between DCM (50 mL) and brine (50 mL). A trace amount of acetic acid was added to neutralize the aqueous solution. The brine phase was additionally extracted with DCM (2 × 50 mL). The combined DCM solution was dried with Na₂SO₄, and the solvent was removed. The obtained white solid was dissolved with THF (10 mL). To this solution, the azido compound **9a–g** (0.75 mmol, 1.5 equiv), catalyst CuIP(OEt)₃ (7 mg, 0.02 mmol, 0.04 equiv), and one drop of DIPEA were added sequentially. The reaction continued overnight at room temperature and was monitored by TLC analysis. Frequently, more and more white precipitate (product) formed as the reaction progressed. The solvent was removed, and the residue was partitioned between DCM (50 mL) and 1% CuSO₄ aqueous solution (50 mL). The aqueous layer was additionally extracted with DCM (2 × 50 mL). The combined DCM layers were dried with Na₂SO₄. After removal of the solvent, the crude product was purified via flash column chromatography to afford the final product **21a–g**.

(E)-3-(1-Benzyl-1H-1,2,3-triazol-4-yl)-N-(4-methoxybenzyloxy) Acrylamide (21a). A white solid was obtained (87%, 158 mg **21a** product from 0.5 mmol **7**) via flash column chromatography (MeOH:DCM, from 1.2:100 to 1.5:100). ¹H NMR (500 MHz, CD₂Cl₂ and CD₃OD): δ 7.91 (s, 1H), 7.50 (d, *J* = 15.7 Hz, 1H), 7.42–7.28 (m, 7H), 6.90 (d, *J* = 8.4 Hz, 2H), 6.54 (d, *J* = 15.7 Hz, 1H), 5.56 (s, 2H), 4.84 (s, 2H), 3.79 (s, 3H). ¹³C NMR (125 MHz, CD₂Cl₂ and CD₃OD): δ 164.8, 160.8, 144.5, 135.4, 131.6, 129.7, 129.4, 129.2, 128.7, 128.3, 125.0, 119.6, 114.4, 78.5, 55.6, 54.8. HRMS (ESI) calcd for C₂₀H₂₀N₄O₃Na [M + Na]⁺ 387.1433, found 387.1431.

(E)-N-(4-Methoxybenzyloxy)-3-(1-phenethyl-1H-1,2,3-triazol-4-yl) Acrylamide (21b). A white solid was obtained (97% yield, 184 mg **21b** from 0.5 mmol **7**) via flash column chromatography (MeOH:DCM, from 0.8:100 to 1.5:100). ¹H NMR (500 MHz, DMF-*d*₇): δ 11.28 (s, 1H), 8.36 (s, 1H), 7.56 (d, *J* = 15.7 Hz, 1H), 7.40 (d, *J* = 8.5 Hz, 2H), 7.35–7.20 (m, 5H), 6.98 (d, *J* = 8.6 Hz, 2H), 6.72 (d, *J* = 15.5 Hz, 1H), 4.89 (s, 2H), 4.74 (t, *J* = 7.3 Hz, 2H), 3.83 (s, 3H), 3.27 (t, *J* = 7.3 Hz, 2H). ¹³C NMR (125 MHz, DMF-*d*₇): δ 164.1, 161.0, 144.2, 138.9, 131.9, 129.9, 129.6, 129.4, 127.7, 125.8, 120.2, 114.7, 78.1, 56.0, 52.0, 37.0. HRMS (ESI) calcd for C₂₁H₂₂N₄O₃Na [M + Na]⁺ 401.1590, found 401.1585.

(E)-N-(4-Methoxybenzyloxy)-3-(1-(3-phenylpropyl)-1H-1,2,3-triazol-4-yl)acrylamide (21c). A white solid was obtained (95% yield, 186 mg **21c** from 0.5 mmol **7**) via flash column chromatography (MeOH:DCM, from 0.8:100 to 1.5:100). ¹H NMR (500 MHz, DMF-*d*₇): δ 11.29 (s, 1H), 8.49 (s, 1H), 7.60 (d, *J* = 15.7 Hz, 1H), 7.40 (d, *J* = 8.5 Hz, 2H), 7.35–7.30 (m, 2H), 7.30–7.25 (m, 2H), 7.25–7.20 (m, 1H), 6.98 (d, *J* = 8.6 Hz, 2H), 6.75 (d, *J* = 15.5 Hz, 1H), 4.90 (s, 2H), 4.50 (t, *J* = 7.3 Hz, 2H), 3.83 (s, 3H), 2.67 (t, *J* = 7.3 Hz, 2H), 2.25 (t, *J* = 7.3 Hz, 2H). ¹³C NMR (125 MHz, DMF-*d*₇): δ 164.1, 161.0, 144.5, 142.2, 131.9, 129.7, 129.6, 129.5, 127.2, 125.8, 120.3, 114.8, 78.1, 56.0, 50.4, 33.3, 32.8 (one peak

less due to overlap). HRMS (ESI) calcd for $C_{22}H_{24}N_4O_3Na$ [$M + Na$] $^+$ 415.1746, found 415.1745.

(*E*)-*N*-(4-Methoxybenzyloxy)-3-(1-(2-phenoxyethyl)-1*H*-1,2,3-triazol-4-yl)acrylamide (**21d**). A white solid was obtained (89% yield, 176 mg **21d** from 0.5 mmol **7**) via flash column chromatography (MeOH:DCM, from 1.0:100 to 2.0:100). 1H NMR (500 MHz, DMF-*d*₇): δ 11.26 (s, 1H), 8.55 (s, 1H), 7.61 (d, $J = 15.7$ Hz, 1H), 7.40 (d, $J = 8.3$ Hz, 2H), 7.36–7.27 (m, 2H), 7.06–6.90 (m, 5H), 6.77 (d, $J = 14.8$ Hz, 1H), 4.91 (t, $J = 5.0$ Hz, 2H), 4.89 (s, 2H), 4.51 (t, $J = 5.1$ Hz, 2H), 3.83 (s, 3H). ^{13}C NMR (125 MHz, DMF-*d*₇): δ 164.2, 161.0, 159.4, 144.5, 131.9, 130.6, 129.6, 129.5, 126.5, 122.3, 120.4, 115.7, 114.8, 78.1, 67.4, 56.0, 50.6. HRMS (ESI) calcd for $C_{21}H_{22}N_4O_4Na$ [$M + Na$] $^+$ 417.1539, found 417.1543.

(*E*)-*N*-(4-Methoxybenzyloxy)-3-(1-(2-oxo-2-phenylethyl)-1*H*-1,2,3-triazol-4-yl)acrylamide (**21e**). A pale-yellow solid was obtained (38% yield, 110 mg **21e** from 0.73 mmol **7**) via flash column chromatography (MeOH:DCM, from 1.5:100 to 2:100). 1H NMR (500 MHz, DMF-*d*₇): δ 11.30 (s, 1H), 8.48 (s, 1H), 8.17 (d, $J = 7.4$ Hz, 2H), 7.78 (t, $J = 7.4$ Hz, 1H), 7.72–7.62 (m, 3H), 7.41 (d, $J = 8.3$ Hz, 2H), 6.99 (d, $J = 8.5$ Hz, 2H), 6.80 (d, $J = 15.6$ Hz, 1H), 6.35 (s, 2H), 4.91 (s, 2H), 3.83 (s, 3H). ^{13}C NMR (125 MHz, DMF-*d*₇): δ 192.3, 163.4, 160.2, 143.8, 134.8, 134.6, 131.1, 129.3, 128.9, 128.7, 128.6, 126.9, 119.7, 114.0, 77.3, 56.4, 55.3. HRMS (ESI) calcd for $C_{21}H_{20}N_4O_4Na$ [$M + Na$] $^+$ 415.1382, found 387.1378.

(*E*)-*N*-(4-Methoxybenzyloxy)-3-(1-(2-oxo-2-(phenylamino)-ethyl)-1*H*-1,2,3-triazol-4-yl)acrylamide (**21f**). A white solid was obtained (92%, 187 mg product **21f** from 0.5 mmol **7**) via flash column chromatography (MeOH:DCM, from 2.5:100 to 3.5:100). 1H NMR (500 MHz, DMF-*d*₇): δ 11.29 (s, 1H), 10.60 (s, 1H), 8.53 (s, 1H), 7.69 (d, $J = 8.0$ Hz, 2H), 7.65 (d, $J = 15.7$ Hz, 1H), 7.41 (d, $J = 8.4$ Hz, 2H), 7.36 (dd, $J_1 = 7.6$ Hz, $J_2 = 8.4$ Hz, 2H), 7.12 (t, $J = 7.4$ Hz, 1H), 6.98 (d, $J = 8.6$ Hz, 2H), 6.78 (d, $J = 15.7$ Hz, 1H), 5.52 (s, 2H), 4.90 (s, 2H), 3.83 (s, 3H). ^{13}C NMR (125 MHz, DMF-*d*₇): δ 164.6, 163.4, 160.2, 143.6, 139.3, 131.1, 129.2, 128.9, 128.7, 126.8, 124.1, 119.6, 114.0, 77.3, 55.2, 52.8 (one peak less due to the overlap). HRMS (ESI) calcd for $C_{21}H_{21}N_5O_4Na$ [$M + Na$] $^+$ 430.1491, found 430.1492.

(*E*)-3-(1-Cinnamyl-1*H*-1,2,3-triazol-4-yl)-*N*-(4-methoxybenzyloxy)acrylamide (**21g**). A white solid was obtained (86% yield, 216 mg product **21g** from 150 mg **7**) via flash column chromatography (MeOH:DCM, from 1.0:100 to 2.0:100). 1H NMR (500 MHz, DMF-*d*₇): δ 11.29 (s, 1H), 8.52 (s, 1H), 7.62 (d, $J = 15.7$ Hz, 1H), 7.53 (d, $J = 7.3$ Hz, 2H), 7.42–7.36 (m, 4H), 7.31 (t, $J_1 = 7.3$ Hz, $J_2 = 2.0$ Hz, 1H), 6.98 (d, $J = 8.6$ Hz, 2H), 6.78 (m, 2H), 6.61 (td, $J_1 = 15.8$ Hz, $J_2 = 6.3$ Hz, 1H), 5.30 (d, $J = 6.1$ Hz, 2H), 4.89 (s, 2H), 3.83 (s, 3H). ^{13}C NMR (125 MHz, DMF-*d*₇): δ 164.1, 161.0, 144.7, 137.3, 135.4, 131.9, 129.8, 129.7, 129.4, 129.3, 127.8, 125.7, 124.5, 120.4, 114.8, 78.1, 56.0, 52.8. HRMS (ESI) calcd for $C_{22}H_{22}N_4O_3Na$ [$M + Na$] $^+$ 413.1590, found 413.1581.

General Procedure for the Preparation of 22a–g. The alkyne precursor **8** (589 mg, 2.12 mmol, 1.0 equiv) was added to a reaction vessel containing THF (50 mL) and MeOH (50 mL). Cesium fluoride (322 mg, 2.12 mmol, 1.0 equiv) was then added, after which the reaction was monitored by TLC analysis. The desilylation intermediate was slightly more polar than **8**. Upon the disappearance of **8**, the solution was split into 10 equal fractions. These fractions were used directly in the ensuing reactions as workup led to degradation of the alkyne. To each fraction of the alkyne solution, the azido compound **9a–g** (0.32 mmol, 1.5 equiv), catalyst $CuIP(OEt)_3$ (10 mg, 0.028 mmol, 0.1 equiv), and one drop of DIPEA were added sequentially. The reaction was allowed to proceed to completion by stirring overnight at room temperature. The solvent was removed, and the residue was partitioned between DCM (50 mL) and 1% $CuSO_4$ aqueous solution (50 mL). The aqueous phase was additionally extracted with DCM (2 \times 50 mL). The combined organic fractions were then dried (Na_2SO_4). After removal of the solvent, the crude product was purified via flash column chromatography.

1-Benzyl-1*H*-[1,2,3]triazole-4-carboxylic Acid (4-Methoxybenzyloxy)-amide (22a). A white solid was obtained (83% yield, 60 mg **22a** from 0.212 mmol **8**) via flash column chromatography (MeOH:DCM, from 0.5:100 to 0.8:100). 1H NMR (500 MHz, DMF-*d*₇): δ 11.76 (bd s, 1H), 8.72 (s, 1H), 7.60–7.25 (m, 7H), 6.96 (d, $J = 7.3$ Hz, 2H), 5.77 (s, 2H), 4.95 (s, 2H), 3.82 (s, 3H). ^{13}C NMR (125 MHz, DMF-*d*₇): δ 161.0, 159.1, 142.8, 137.1, 131.8, 130.0, 129.5, 129.3, 127.7, 114.7, 78.5, 56.0, 54.5. HRMS (ESI) calcd for $C_{18}H_{18}N_4O_3Na$ [$M + Na$] $^+$ 361.1277, found 361.1263.

1-Phenethyl-1*H*-[1,2,3]triazole-4-carboxylic Acid (4-Methoxybenzyloxy)-amide (22b). A white solid was obtained (95% yield, 63 mg **22b** from 0.189 mmol **8**) via flash column chromatography (MeOH:DCM, from 0.5:100 to 0.75:100). 1H NMR (500 MHz, DMF-*d*₇): δ 11.69 (bd s, 1H), 8.56 (s, 1H), 7.42 (d, $J = 8.6$ Hz, 2H), 7.32–7.20 (m, 5H), 6.96 (d, $J = 8.7$ Hz, 2H), 4.93 (s, 2H), 4.77 (t, $J = 7.3$ Hz, 2H), 3.81 (s, 3H), 3.28 (t, $J = 7.4$ Hz, 2H). ^{13}C NMR (125 MHz, DMF-*d*₇): δ 161.0, 142.4, 138.8, 131.8, 129.9, 129.6, 129.3, 127.8, 127.7, 114.8, 78.5, 56.0, 52.2, 37.0. HRMS (ESI) calcd for $C_{19}H_{20}N_4O_3Na$ [$M + Na$] $^+$ 375.1433, found 375.1425.

1-(3-Phenyl-propyl)-1*H*-[1,2,3]triazole-4-carboxylic Acid (4-Methoxybenzyloxy)-amide (22c). A white solid was obtained (67% yield, 53 mg **22c** from 0.212 mmol **8**) via flash column chromatography (MeOH:DCM, from 0.5:100 to 0.6:100). 1H NMR (500 MHz, DMF-*d*₇): δ 11.74 (bd s, 1H), 8.69 (s, 1H), 7.45 (d, $J = 8.4$ Hz, 2H), 7.36–7.20 (m, 5H), 6.98 (d, $J = 8.5$ Hz, 2H), 4.97 (s, 2H), 4.54 (t, $J = 7.0$ Hz, 2H), 3.83 (s, 3H), 2.67 (t, $J = 7.7$ Hz, 2H), 2.27 (tt, $J_1 = J_2 = 7.4$ Hz, 2H). ^{13}C NMR (125 MHz, DMF-*d*₇): δ 161.0, 159.2, 142.6, 142.1, 131.8, 129.5, 129.3, 127.6, 127.2, 114.8, 78.5, 56.0, 50.7, 33.3, 32.8 (one less peak due to overlap). HRMS (ESI) calcd for $C_{20}H_{22}N_4O_3Na$ [$M + Na$] $^+$ 389.1590, found 389.1585.

1-(2-Phenoxy-ethyl)-1*H*-[1,2,3]triazole-4-carboxylic Acid (4-Methoxybenzyloxy)-amide (22d). A white solid was obtained (56% yield, 44 mg **22d** from 0.212 mmol **8**) via flash column chromatography (MeOH:DCM, from 0.5:100 to 1.0:100). 1H NMR (500 MHz, DMF-*d*₇): δ 11.81–11.72 (bd s, 1H), 8.73 (s, 1H), 7.44 (d, $J = 8.6$ Hz, 2H), 7.31 (t, $J = 8.0$ Hz, 2H), 7.01–6.95 (m, 5H), 4.98–4.94 (m, 4H), 4.54 (t, $J = 5.2$ Hz, 2H), 3.82 (s, 3H). ^{13}C NMR (125 MHz, DMF-*d*₇): δ 161.0, 159.4, 159.1, 142.6, 131.8, 130.7, 129.3, 128.2, 122.3, 115.7, 114.7, 78.5, 63.7, 56.0, 50.8. HRMS (ESI) calcd for $C_{19}H_{20}N_4O_4Na$ [$M + Na$] $^+$ 391.1382, found 391.1379.

1-(2-oxo-2-Phenyl-ethyl)-1*H*-[1,2,3]triazole-4-carboxylic Acid (4-Methoxybenzyloxy)-amide (22e). A pale-yellow solid was obtained (76% yield, 74 mg **22e** from 0.265 mmol **8**) via flash column chromatography (MeOH:DCM, from 0.25:100 to 1:100). 1H NMR (500 MHz, DMF-*d*₇): δ 11.83 (s, 1H), 8.69 (s, 1H), 8.17 (d, $J = 7.6$ Hz, 2H), 7.78 (t, $J = 7.3$ Hz, 1H), 7.65 (dd, $J_1 = J_2 = 7.5$ Hz, 2H), 7.46 (d, $J = 8.2$ Hz, 2H), 6.99 (d, $J = 8.2$ Hz, 2H), 6.39 (s, 2H), 4.99 (s, 2H), 3.84 (s, 3H). ^{13}C NMR (125 MHz, DMF-*d*₇): δ 192.9, 161.0, 159.2, 142.6, 135.6, 135.4, 131.9, 130.1, 129.5, 129.3, 114.8, 78.5, 57.4, 56.0 (one less peak due to overlap). HRMS (ESI) calcd for $C_{19}H_{18}N_4O_4Na$ [$M + Na$] $^+$ 389.1266, found 389.1218.

1-Phenylcarbamoylmethyl-1*H*-[1,2,3]triazole-4-carboxylic Acid (4-Methoxybenzyloxy)-amide (22f). The crude product was dissolved in a minimal amount of 5% MeOH in DCM. The pure compound was then precipitated via addition of hexane (2:1 = hexane:solution). Following centrifugation (5000 rpm, 5 min), the supernatant was removed and the solid was sonicated in the presence of a 1% EDTA aqueous solution. The solution was then filtered to afford the pure compound (81% yield, 82 mg **22f** from 0.265 mmol **8**). 1H NMR (500 MHz, DMF-*d*₇): δ 11.90–11.70 (bd s, 1H), 10.65 (s, 1H), 8.72 (s, 1H), 7.69 (d, $J = 8.0$ Hz, 2H), 7.45 (d, $J = 8.5$ Hz, 2H), 7.36 (dd, $J_1 = J_2 = 7.8$ Hz, 2H), 7.12 (t, $J = 7.3$ Hz, 1H), 6.98 (d, $J = 8.5$ Hz, 2H), 5.57 (s, 2H), 4.98 (s, 2H), 3.83 (s, 3H). ^{13}C NMR (125 MHz, DMF-*d*₇): δ 165.2, 161.0, 159.2, 142.4, 140.0, 131.8, 129.4, 129.3, 124.9, 120.4, 114.8, 78.5, 56.0, 53.7 (one less peak due to overlap). HRMS (ESI) calcd for $C_{19}H_{19}N_5O_4Na$ [$M + Na$] $^+$ 404.1335, found 404.1319.

1-(3-Phenyl-allyl)-1H-[1,2,3]triazole-4-carboxylic Acid (4-Methoxy-benzyloxy)-amide (22g). A white solid was obtained (80% yield, 62 mg of **22g** from 0.212 mmol **8**) via flash column chromatography (MeOH:DCM, from 0.25:100 to 0.5:100). ^1H NMR (500 MHz, DMF- d_7): δ 11.76 (s, 1H), 8.69 (s, 1H), 7.54 (d, J = 7.4 Hz, 2H), 7.44 (d, J = 8.6 Hz, 2H), 7.38 (dd, $J_1 = J_2 = 7.5$ Hz, 2H), 7.31 (t, J = 7.3 Hz, 1H), 6.97 (d, J = 8.5 Hz, 2H), 6.80 (d, J = 15.9 Hz, 1H), 6.63 (td, $J_1 = 15.8$ Hz, $J_2 = 6.6$ Hz, 1H), 5.34 (d, J = 6.5, 2H), 4.96 (s, 2H), 3.82 (s, 3H). ^{13}C NMR (125 MHz, DMF- d_7): δ 161.0, 159.1, 142.7, 137.3, 135.6, 131.8, 129.8, 129.4, 129.3, 127.8, 127.5, 124.4, 114.7, 78.5, 56.0, 53.0. HRMS (ESI) calcd for $\text{C}_{20}\text{H}_{20}\text{N}_4\text{O}_3\text{Na}$ [$\text{M} + \text{Na}$] $^+$ 387.1433, found 387.1430.

Acknowledgment. This project was supported by The Ohio State University (support to Peng George Wang). The Cell Line Studies were performed by the NIH.

Supporting Information Available: Proton and carbon NMR spectra of new compounds. This material is available free of charge via the Internet at <http://pubs.acs.org>.

References

- Kouzarides, T. Chromatin modifications and their function. *Cell* **2007**, *128*, 693–705.
- Bernstein, B. E.; Meissner, A.; Lander, E. S. The mammalian epigenome. *Cell* **2007**, *128*, 669–681.
- Li, E. Chromatin modification and epigenetic reprogramming in mammalian development. *Nat. Rev. Genet.* **2002**, *3*, 662–673.
- Trojer, P.; Reinberg, D. Histone lysine demethylases and their impact on epigenetics. *Cell* **2006**, *125*, 213–217.
- Yang, X. J.; Seto, E. The Rpd3/Hda1 family of lysine deacetylases: from bacteria and yeast to mice and men. *Nat. Rev. Mol. Cell Biol.* **2008**, *9*, 206–218.
- Wolffe, A. P. Histone deacetylase: a regulator of transcription. *Science* **1996**, *272*, 371–372.
- Lin, R. J.; Sternsdorf, T.; Tini, M.; Evans, R. M. Transcriptional regulation in acute promyelocytic leukemia. *Oncogene* **2001**, *20*, 7204–7215.
- Dokmanovic, M.; Marks, P. A. Prospects: Histone deacetylase inhibitors. *J. Cell. Biochem.* **2005**, *96*, 293–304.
- Drummond, D. C.; Nobel, C. O.; Kirpotin, D. B.; Guo, Z.; Scott, G. K.; Benz, C. C. Clinical development of histone deacetylase inhibitors as anticancer agents. *Annu. Rev. Pharmacol. Toxicol.* **2005**, *45*, 495–528.
- Luo, J.; Su, F.; Chen, D.; Shiloh, A.; Gu, W. Deacetylation of p53 modulates its effect on cell growth and apoptosis. *Nature* **2000**, *408*, 377–381.
- Johnstone, R. W.; Licht, J. D. Histone deacetylase inhibitors in cancer therapy: Is transcription the primary target? *Cancer Cell* **2003**, *4*, 13–18.
- Nusinzon, I.; Horvath, C. M. Interferon-stimulated transcription and innate antiviral immunity require deacetylase activity and histone deacetylase 1. *Proc. Natl. Acad. Sci. U.S.A.* **2003**, *100*, 14742–14747.
- Yuan, Z.-L.; Guan, Y.-J.; Chatterjee, D.; Chin, Y. E. Stat3 Dimerization regulated by reversible acetylation of a single lysine residue. *Science* **2005**, *307*, 269–273.
- Chen, L.-F.; Fischle, W.; Verdin, E.; Greene, W. C. Duration of nuclear NF- κ B action regulated by reversible acetylation. *Science* **2001**, *307*, 269–273.
- Gu, W.; Roeder, R. G. Activation of p-53 sequence-specific DNA binding by acetylation of the p53 C-terminal domain. *Cell* **1997**, *90*, 595–606.
- Martinez-Balbas, M. A.; Bauer, U. M.; Nielsen, S. J.; Brehm, A.; Kouzarides, T. Regulation of E2F1 activity by acetylation. *EMBO J.* **2000**, *19*, 662–671.
- Cohen, H. Y.; Lavu, S.; Bitterman, K. J.; Hekking, B.; Imahiyerobo, T. A.; Miller, C.; Frye, R.; Ploegh, H.; Kessler, B. M.; Sinclair, D. A. Acetylation of the C terminus of Ku70 by CBP and PCAF controls Bax-mediated apoptosis. *Mol. Cell* **2004**, *13*, 627–638.
- Pan, L.; Lu, J.; Huang, B. HDAC inhibitors: a potential new category of anti-tumor agents. *Cell. Mol. Immunol.* **2007**, *4*, 337–343.
- Dokmanovic, M.; Clarke, C.; Marks, P. A. Histone deacetylase inhibitors: overview and perspectives. *Mol. Cancer Res.* **2007**, *5*, 981–989.
- Bolden, J. E.; Peart, M. J.; Johnstone, R. W. Anticancer activities of histone deacetylase inhibitors. *Nat. Rev. Drug Discovery* **2006**, *5*, 769–784.
- Minucci, S.; Pelicci, P. G. Histone deacetylase inhibitors and the promise of epigenetic (and more) treatments for cancer. *Nat. Rev. Cancer* **2006**, *6*, 38–51.
- Finnin, M. S.; Donigan, J. R.; Cohen, A.; Richon, V. M.; Rifkind, R. A.; Marks, P. A.; Breslow, R.; Pavlathich, N. P. Structures of a histone deacetylase homologue bound to the TSA and SAHA inhibitors. *Nature* **1999**, *401*, 188–193.
- Elaut, G.; Laus, G.; Alexandre, E.; Richert, L.; Bachellier, P.; Tourwe, D.; Rogiers, V.; Vanhaecke, T. A metabolic screening study of trichostatin A (TSA) and TSA-like histone deacetylase inhibitors in rat and human primary hepatocyte cultures. *J. Pharmacol. Exp. Ther.* **2007**, *321*, 400–408.
- Sanderson, L.; Taylor, G. W.; Aboagye, E. O.; Alao, J. P.; Latigo, J. R.; Coombes, R. C.; Vigushin, D. M. Plasma pharmacokinetics and metabolism of the histone deacetylase inhibitor trichostatin A after intraperitoneal administration of mice. *Drug Metab. Dispos.* **2004**, *32*, 1132–1138.
- Elaut, G.; Toeroek, G.; Papeleu, P.; Vanhaecke, T.; Laus, G.; Tourwe, D.; Rogiers, V. Rat hepatocyte suspensions as a suitable in vitro model for studying the biotransformation of histone deacetylase inhibitors. *ATLA, Altern. Lab. Anim.* **2004**, *32*, 105–112.
- Suzuki, T.; Miyata, N. Rational design of non-hydroxamate histone deacetylase inhibitors. *Mini-Rev. Med. Chem.* **2006**, *6*, 515–526.
- Suzuki, T.; Miyata, N. Non-hydroxamate histone deacetylase inhibitors. *Curr. Med. Chem.* **2005**, *12*, 2867–2880.
- Forumai, R.; Komatsu, Y.; Nishino, N.; Khochbin, S.; Yoshida, M.; Horinouchi, S. Potent histone deacetylase inhibitors built from trichostatin A and cyclic tetrapeptide antibiotics including trapoxin. *Proc. Natl. Acad. Sci. U.S.A.* **2001**, *98*, 87–92.
- Jones, P.; Altamura, S.; Chakravarty, P. K.; Cecchetti, O.; DeFrancesco, R.; Gallinari, P.; Ingenito, R.; Meinke, P. T.; Petrocchi, A.; Rowley, M. A series of novel, potent and selective histone deacetylase inhibitors. *Bioorg. Med. Chem. Lett.* **2006**, *16*, 5948–5952.
- Kahnberg, P.; Lucke, A. J.; Glenn, M. P.; Boyle, G. M.; Tyndall, J. D. A.; Parsons, P. G.; Fairlie, D. P. Design, synthesis, potency and cytoselectivity of anticancer agents derived by parallel synthesis from aminosuberlic acid. *J. Med. Chem.* **2006**, *49*, 7611–7622.
- Vannini, A.; Volpari, C.; Filocamo, G.; Casavola, E. C.; Brunetti, M.; Renzoni, D.; Chakravarty, P.; Paolini, C.; De Francesco, R.; Gallinari, P.; et al. Crystal structure of a eukaryotic zinc-dependent histone deacetylase, human HDAC8, complexed with a hydroxamic acid inhibitor. *Proc. Natl. Acad. Sci. U.S.A.* **2004**, *101*, 15064–15069.
- Kolb, H. C.; Finn, M. G.; Sharpless, K. B. Click chemistry: diverse chemical function from a few good reactions. *Angew. Chem., Int. Ed.* **2001**, *40*, 2004–2021. (b) Moses, J. E.; Moorhouse, A. D. The growing applications of click chemistry. *Chem. Soc. Rev.* **2007**, *36*, 1249–1262.
- Roper, S.; Kolb, H. C. Click chemistry for drug discovery. *MethodsPrinciples Med. Chem.* **2006**, *34*, 313–339.
- Weber, L. In vitro combinatorial chemistry to create drug candidates. *Drug Discovery Today: Technol.* **2004**, *1*, 261–267.
- Kolb, H. C.; Sharpless, K. B. The growing impact of click chemistry on drug discovery. *Drug Discovery Today* **2003**, *8*, 1128–1137.
- Alvarez, S. G.; Alvarez, M. T. A practical procedure for the synthesis of alkyl azides at ambient temperature in dimethyl sulfoxide in high purity and yield. *Synthesis* **1997**, 413–414.
- Ramsay, S. L.; Freeman, C.; Grace, P. B.; Redmond, J. W.; MacLeod, J. K. Mild tagging procedures for the structural analysis of glycans. *Carbohydr. Res.* **2001**, *33*, 59–71.
- Dixon, D. J.; Ley, S. V.; Longbottom, D. A. Copper(I)-catalyzed preparation of (*E*)-3-iodoprop-2-enoic acid. *Org. Synth.* **2003**, *80*, 129–132.
- Eichberg, M. J.; Dorta, R. L.; Lamotte, K.; Vollhardt, K. P. C. The formal total synthesis of (\pm)-strychnine via a cobalt-mediated [2 + 2] cycloaddition. *Org. Lett.* **2000**, *2*, 2479–2481.
- Krusche, C. A.; Wuelfing, P.; Kersting, C.; Vloet, A.; Boecker, W.; Kiesel, L.; Beier, H. M.; Alfer, J. Histone deacetylase-1 and -3 protein expression in human breast cancer: a tissue microarray analysis. *Breast Cancer Res. Treat.* **2005**, *90*, 15–23.
- Park, J.-H.; Jung, Y.; Kim, T. Y.; Kim, S. G.; Jong, H.-S.; Lee, J. W.; Kim, D.-K.; Lee, J.-S.; Kim, N. K.; Kim, T.-Y.; Bang, Y.-J. Class I Histone Deacetylase-Selective Novel Synthetic Inhibitors Potentially Inhibit Human Tumor Proliferation. *Clin. Cancer Res.* **2004**, *10*, 5271–5281.
- Halkidou, K.; Gaughan, L.; Cook, S.; Leung, H. Y.; Neal, D. E.; Robson, C. N. Upregulation and nuclear recruitment of HDAC1 in hormone refractory prostate cancer. *Prostate* **2004**, *59*, 177–189.
- Choi, J.-H.; Kwon, H. J.; Yoon, B.-I.; Kim, J.-H.; Han, S. U.; Joo, H. J.; Kim, D.-Y. Expression profile of histone deacetylase 1 in gastric cancer tissues. *Jpn. J. Cancer Res.* **2001**, *92*, 1300–1304.
- Waltregny, D.; North, B.; Van Mellaert, F.; de Leval, J.; Verdin, E.; Castronovo, V. Screening of histone deacetylases (HDAC) expression in human prostate cancer reveals distinct class I HDAC profiles

- between epithelial and stromal cells. *Eur. J. Histochem.* **2004**, *48*, 273–290.
- (45) KrennHrubec, K.; Marshall, B. L.; Hedglin, M.; Verdin, E.; Ulrich, S. M. Design and evaluation of “Linkerless” hydroxamic acids as selective HDAC8 inhibitors. *Bioorg. Med. Chem. Lett.* **2007**, *17*, 2874–2878.
- (46) Hu, E.; Dul, E.; Sung, C.-M.; Chen, Z.; Kirkpatrick, R.; Zhang, G.-F.; Johanson, K.; Liu, R.; Lago, A.; Hofmann, G.; et al. Identification of novel isoform-selective inhibitors within class I histone deacetylases. *J. Pharmacol. Exp. Ther.* **2003**, *307*, 720–728.
- (47) These NSC numbers were assigned by the NCI.
- (48) Shoemaker, R. H. The NCI60 human tumour cell line anticancer drug screen. *Nat. Rev. Cancer* **2006**, *6*, 813–823.
- (49) It should be noted that the NCI does not include an error analysis in their reports of compound activity in the human cancer cell line screen. However, they do perform an adequate number of determinations. Specifically, two microtiter plates are utilized for the testing of each cell line. Each drug is then tested at five concentrations along with a control. Furthermore, this screen is also well established at the NCI as it became operational in 1990 following a five year development period.
- (50) Katritzky, A. R.; Liso, G.; Lunt, E.; Patel, R. C.; Thind, S. S.; Zia, A. Heterocycles in organic synthesis. Part 42. Preparation of azides, phthalimides and sulfonamides from primary amines. *J. Chem. Soc., Perkin Trans. 1* **1980**, 849–850.
- (51) Benati, L.; Bencivenni, G.; Leardini, R.; Nanni, D.; Minozzi, M.; Spagnolo, P.; Scialpi, R.; Zanardi, G. Reaction of azides with dichloroindium hydride: very mild production of amines and pyrrolidin-2-imines through possible indium-aminy radicals. *Org. Lett.* **2006**, *8*, 2499–2502.
- (52) Mandel, S. M.; Bauer, J. A. K.; Gudmundsdottir, A. D. Photolysis of α -azidoacetophenones: trapping of triplet alkyl nitrenes in solution. *Org. Lett.* **2001**, *3*, 523–526.
- (53) Srinivasan, R.; Uttamchandani, M.; Yao, S. Q. Rapid assembly and in situ screening of bidentate inhibitors of protein tyrosine phosphatases. *Org. Lett.* **2006**, *8*, 713–716.

JM8005355